Dalton
www.rsc.org/dalton

Solution structure and behaviour of Δ-*cis*-α-[Ru(*R*,*R*-picchxnMe$_2$)(phi)]$^{2+}$ by NMR spectroscopy and molecular modelling †

Emma M. Proudfoot,[a] Joel P. Mackay[b] and Peter Karuso*[a]

[a] *Department of Chemistry, Macquarie University, NSW, 2109, Australia. E-mail: Peter.Karuso@mq.edu.au*

[b] *Department of Biochemistry, University of Sydney, NSW, 2006, Australia*

Received 11th September 2002, Accepted 25th November 2002
First published as an Advance Article on the web 17th December 2002

The self-association of the DNA metalloprobe Δ-*cis*-α-[Ru(*R*,*R*-picchxnMe$_2$)(phi)]$^{2+}$ (α-phi) in aqueous solution has been investigated using ^{1}H NMR spectroscopy and molecular modelling. The concentration dependence of proton chemical shifts of the complex gave initial indications of a self-associated species, while its structural isomer Δ-*cis*-β-[Ru(*R*,*R*-picchxnMe$_2$)(phi)]$^{2+}$ (β-phi) showed no such dependence. 2D-COSY and 2D-ROESY experiments were used for the complete assignment of the proton resonances of both isomers and allowed a qualitative determination of the self-association of the α isomer through the detection of intermolecular ROEs. NMR spectroscopy can also be effectively used to differentiate Δ- and Λ-diastereomers. In addition, we show, by pulsed field gradient longitudinal eddy-current delay (PFGLED) NMR spectroscopy, that α-phi self-associates at higher concentrations with an effective molecular weight at 25 mM three times that at 2.5 mM. This apparent oligomerisation was not observed for the β-isomer.

Introduction

The interactions between π-systems control the vertical base–base interactions in DNA. This π–π stacking phenomenon can also be observed in the packing of aromatic molecules in crystals[1–3] and in solution,[4–8] where it serves to avoid the disruption of solvent–solvent interactions. The electrostatic effects (π–σ attraction *vs.* π–π repulsion) dictate the geometry of the stacking, while van der Waals interactions and solvophobic effects (especially in water) determine the magnitude of the stacking interaction.[9] Aromatic stacking in D_2O was observed for Ru complexes based on the Δ-*cis*-α- and Δ-*cis*-β-[Ru(*R*,*R*-picchxnMe$_2$)(bidentate)]$^{2+}$ template and has previously been noted for Δ-*cis*-α-[Ru(*R*,*R*-picchxnMe$_2$)-(dpq)]$^{2+}$.[10] ‡

Metal complexes incorporating the phi ligand have been shown to be avid DNA intercalators,[11,12] and the metalloprobes Δ-*cis*-α- and Δ-*cis*-β-[Ru(*R*,*R*-picchxnMe$_2$)(phi)]$^{2+}$ exhibit similar qualities.[13] In order to understand the full nature of their interactions in solution with both DNA and their own species, it is important to investigate the nature of the observed self-association. The picchxnMe$_2$ tetradentate ligand[14] is based on the picen (1,6-bis(2-pyridyl)-2,5-diazahexane) template, recently reviewed by Vagg and co-workers.[15] A tetradentate ligand of this type can form two stereoisomers upon coordination to a Ru^{2+} centre, termed *cis*-α and *cis*-β (Fig. 1). The symmetric *cis*-α form exhibits a C_2-axis, while the asymmetric *cis*-β form has C_1 symmetry.

In this paper, we describe the solution structure of α-phi and compare the concentration dependent behaviour of the α- and β- isomers using NMR spectroscopic titrations, ROESY and PFGLED NMR experiments. These data, in conjunction with restrained MD–MM calculations resulted in quantitative monomer structures comparable to X-ray structures of related complexes and qualitative oligomeric structures.

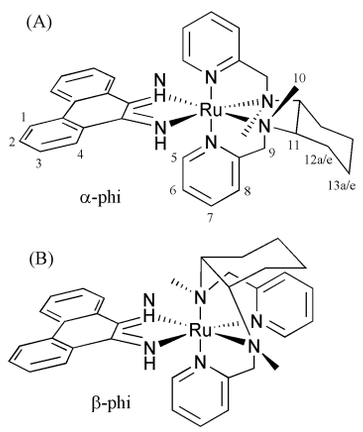

Fig. 1 Structure of (A) Δ-*cis*-α- and (B) Δ-*cis*-β-[Ru(*R*,*R*-picchxnMe$_2$)(phi)]$^{2+}$ showing the ^{1}H numbering scheme used.

Pulsed-field-gradient theory

It is possible to measure the molecular weight of the molecules in solution using Pulsed Field Gradient Longitudinal Eddy-current Delay (PFGLED) NMR spectroscopy. This technique was introduced by Stejskal and Tanner,[16] and has since been used for the study of a variety of samples ranging from small molecules to proteins.[17–19] A series of one-dimensional PFGLED spectra are recorded in which the delay periods (τ, Δ, T and T_e) and the magnitude of the magnetic field gradient pulse are held constant, but the length of the field gradient pulses (δ) is incremented. As the length of the field gradient pulses increases, the signal intensities decrease due to diffusion of the solute through the sample. The rate of decrease and, therefore, the rate of diffusion can be quantified since the spin-echo delay time (τ) and the total length of the pulse sequence are the same for all experiments. The diminution in signal intensity is solely attributed to molecular diffusion,[17] and the molecular weight of the diffusing species can be determined.

The expression that relates signal intensity (R) to the gradient strength (G) and the diffusion coefficient (D_T) is given by eqn. (1).[16]

† Electronic supplementary information (ESI) available: NMR spectra and selected NMR data. See http://www.rsc.org/suppdata/dt/b2/b208846k/

‡ Abbreviations: picchxnMe$_2$ = *N*,*N*′-dimethyl-*N*,*N*′-di(2-picolyl)-1,2-diaminocyclohexane, dpq = dipyrido[3,2-*f*:2′,3′-*h*]quinoxaline, phi = 9,10-phenanthrenequinonediimine, dpqC = dipyrido[3,2-*a*:2′,3′-*c*]-6,7,8,9-tetrahydrophenazine, α-phi = Δ-*cis*-α-[Ru(*R*,*R*-picchxnMe$_2$)-(phi)]$^{2+}$, β-phi = Δ-*cis*-β-[Ru(*R*,*R*-picchxnMe$_2$)(phi)]$^{2+}$, α-dpqC = Λ-*cis*-α-[Ru(*S*,*S*-picchxnMe$_2$)(dpqC)]$^{2+}$.

DOI: 10.1039/b208846k

$$R = \exp(-\gamma^2 G^2 D_T \delta^2 (\Delta - \delta/3)) \quad (1)$$

The translational diffusion coefficient (D_T) is related to the molecular weight of the species according to eqn. (2).[20]

$$MW = \left(\frac{kT}{6\pi\eta F D_T}\right)^3 \left(\frac{4\pi N_A}{3\left[\bar{\nu}_2 + \delta_1 \bar{\nu}_1\right]}\right) \quad (2)$$

Materials and methods

The phi complexes were synthesised by K. Vickery (Macquarie University) and the synthesis of the analogous phen complexes has been described previously.[21] Substitution of the bidentate ligand phen with phi gives an isomeric mixture of Δ-*cis*-α- and Δ-*cis*-β-[Ru(*R*,*R*-picchxnMe$_2$)(phi)]Cl$_2$ that can be separated by chromatography on SP-Sephadex C-25 (NaCl gradient 0–1.3 M). Each complex was freed of salt by lyophilisation and trituration with dichloromethane, exchanged twice with D_2O (99.9%, Aldrich), and then made up in D_2O (500 μl; 99.96% Aldrich) or H_2O with 10% D_2O. 3-(Trimethylsilyl)-1-propanesulfonic acid (TSP) was added as an internal chemical shift reference.

NMR spectra were obtained using Varian XL400 (400 MHz) and Bruker AMX600 or DMX600 (600 MHz) NMR spectrometers. One-dimensional (1D) spectra were recorded with either 16K or 32K data points and zero filled to 64K. Relaxation delays of 1–2 s were employed. Spectral widths were adjusted to allow ~1 ppm either side of the observable resonances and the carrier frequency was set to the solvent signal. Suppression of the residual solvent signal was generally achieved by selective irradiation during the relaxation delay. Spectra in H_2O were acquired using watergate 3–9–19 solvent suppression.[22]

All two-dimensional (2D) spectra were recorded with quadrature detection in both dimensions using time proportional phase incrementation (TPPI). For DQF-COSY and ROESY[23–25] experiments, 2048 data points were collected in t_2 and 512 in t_1, and between 24 and 80 transients were collected at each increment. Relaxation delays and solvent suppression were as for the 1D spectra. ROESY spectra were recorded with a continuous wave pulse equivalent to a 4 KHz spinlock of 10–300 ms.

Data were processed using the Bruker xwinnmr (version 1.3) software. The spectra were zero-filled twice in F1 and once in F2 and processed with either squared sine-bell (π/2- or π/3-shifted) or Lorentzian-Gaussian window functions. The spectra were referenced and phased in both dimensions. A baseline correction was subsequently applied in F2 and if necessary, t_1 noise was subtracted using the Bruker program Aurelia (2.0.6).

The chemical shifts of the aromatic protons of Δ-*cis*-α- and Δ-*cis*-β-[Ru(*R*,*R*-picchxnMe$_2$)(phi)]$^{2+}$ were recorded at 25 °C and plotted as a function of complex concentration in the range 2.5–25 mM. DQF-COSY and ROESY data were collected for the α and β isomers for initial assignment purposes. A series of compensated ROESY spectra were measured for Δ-*cis*-α-[Ru(*R*,*R*-picchxnMe$_2$)(phi)]$^{2+}$ (25 mM, 5 °C) with mixing times of 10, 30, 50, 100, 150, 200 and 300 ms. ROE build-up curves were plotted for five cross peaks (see ESI).

A PFGLED experiment was performed for an H_2O sample, which has a known value of D_T (2.299×10^{-9} m^2 s^{-1}), in order to calibrate the magnitude of the magnetic field gradient pulses (G). The experiment was then repeated for Δ-*cis*-α-[Ru(*R*,*R*-picchxnMe$_2$)(phi)]$^{2+}$ samples at 2.5 and 25 mM, so as to calculate the translational diffusion coefficient, D_T, at each concentration. Shigemi NMR microcells (Wilmad, Buena, NJ) were used so that the entire sample was affected by the gradient. In total, 11 spectra were collected on each of the H_2O and the two complex samples. The initial value of δ (23 μs) was incremented by 1 ms for each spectrum. Accordingly, δ_e was decremented by 1 ms for each spectrum to produce a constant-time experiment. The value for Δ remained unchanged (41 ms). Following acquisition, each spectrum was baseline corrected, 5 Hz of line broadening applied and the same phase correction applied to each spectrum. For each of the complex samples, the intensity of three peaks was measured using the same data point in each spectrum. Using the data for the H_2O sample, a three-parameter exponential curve fit of the form $R_{obs} = R_\infty + R_0 \exp(-G^2 x)$, (where R_0 and R_∞ are the normalised resonance intensities at zero and infinite time, respectively), using $x = \gamma^2 G^2 \delta^2 (\Delta - \delta/3)$ as the independent variable, yielding G. This value of G was then used in exponential curve fits of the form $R_{obs} = R_\infty + R_0 \exp(-D_T x)$ for the *phi* complex, using $x = \gamma^2 G^2 \delta^2 (\Delta - \delta/3)$ as the independent variable. In this way, a value of D_T was obtained for samples at 2.5 and 25 mM.

For the solution structures, a 2D watergate compensated ROESY NMR spectrum (10 % D_2O, 2.5 mM, τ_m = 100 ms, 15 °C) was recorded. ROE cross peaks were selected and integrated and corrected for offset effects.[25] As the methyl groups contain three equivalent protons, that interchange in identity due to rotation about the attached C–C bond, a pseudoatom, equidistant from the three protons was used for ROE distance calculations. All methyl-proton integration volumes were thus divided by 3 and 0.1 Å added to the calculated distance to account for the use of pseudoatoms. Interproton distances were derived using the average volume of the geminal proton cross peaks (12a–12e, 13a–13e) for calibration (1.78 Å). Since α-phi has C_2 symmetry, the constraints were applied in pairs symmetrically. Molecular dynamics and minimisation were performed using the Insight II/Discover3 molecular modelling system.[26] The complex was built using the Builder module in InsightII, and energy minimised briefly. Molecular dynamics simulations were performed at 1000 K for 0.2 ns and a structure sampled every 10 ps in order to generate 20 random structures. The NMR derived distance restraints were then applied using a flat-bottomed potential with an energy penalty of 1000 kcal mol^{-1} Å^{-2} applied outside the upper and lower (± 5%) restraint boundaries. Each structure was cooled to 200 K over 8 ps using a simulated annealing approach.[27] This was followed by minimisation of each structure, involving steepest descents, conjugate gradients and quasi-Newton-Raphson minimisation until the final maximum derivative was less than 0.0001 kcal mol^{-1} Å^{-1}. The ESFF forcefield was used in all Discover3 calculations.[28] A similar approach was used for the dimer structure except the ROESY spectrum was run at 5 °C (τ_m = 30 ms) and no MD calculations were performed.

Results and discussion

NMR solution structure of α-phi

NMR spectroscopy has proved accurate and efficient for the structure determination of information-rich molecules such as proteins and nucleic acids, comparable and complementary to X-ray crystallography.[29,30] However, it has not generally been used for the structure determination of metal complexes, which often have few protons, though there are several examples of the characterisation of inorganic complexes using a combination of NMR spectroscopy and molecular modelling.[31,32] The ESFF (Extensible Systematic Force Field)[28] is useful for metal complexes and organometallics because it has been parameterised for all elements up to radon and gives specific consideration to the coordination geometry of metal complexes.

For the solution structure of α-phi, various ROE cross peaks were omitted from the integration procedure, namely all 9a cross peaks, which were affected by the residual water peak; all coupled cross peaks in the aromatic region and the 9e–14 cross peak, which was originally included in the dynamics/ minimisation but was later removed due to spin diffusion from 9a to 9e.

Table 1 Distance restraints used for the solution structure of Δ-*cis*-α-[Ru(*R*,*R*-picchxnMe$_2$)(phi)]$^{2+}$ using H13a–H13e and H12a–H12e for calibration (1.78 Å)

Cross peak	Average distance calculated from ROE intensity (±5%)/Å	Solution structure distance/Å	
		Δ-Isomer	Λ-Isomer
H13e–H12e	2.40–2.66	2.48	2.48
H12a–H10	2.57–2.84	2.70	2.98
H12e–H10	3.18–3.52	3.47	3.87
H10–H9e	2.94–3.24	3.10	3.55
H11–H9e	2.79–3.09	2.79	3.20
H12e–H9e	2.42–2.68	2.42	2.10
H10–H5	2.96–3.28	3.28	3.55
H11–H8	3.45–3.81	3.81	3.51
H8–H9e	2.58–2.86	2.58	2.67
H10–H14	3.29–3.63	3.48	3.07
H5–H14	2.63–2.91	2.90	3.00
H4–H14	1.99–2.19	1.99	2.15

The 9e cross peaks were taken from one side of the diagonal only, as they were also affected by the residual water peak. Atoms that were within 4 Å of their symmetry related atoms were also omitted from the structure calculation. For example, the methyl (H10) was ~3 Å from H11 and the symmetry related H11.

The ROE restrained simulated annealing protocol yielded 20 minimised structures. Superposition of all 20 structures revealed that they were virtually identical, indicating that there was only one stable solution conformation consistent with the observed ROEs, and Fig. 2 shows the geometry of the average

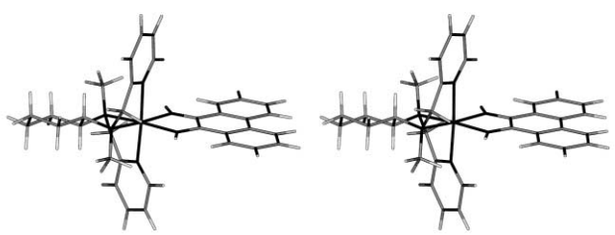

Fig. 2 Stereoview of the average NMR solution structure of Δ-*cis*-α-[Ru(*R*,*R*-picchxnMe$_2$)(phi)]$^{2+}$.

structure. Table 1 shows the distance restraints derived from the observed ROEs (see ESI), and the actual distance in the final solution structure. All distances refined to within or equal to the ± 5% limit imposed by the distance restraint range.

Restrained MD-MM was also easily able to differentiate Δ- and Λ-isomers: For α-phi, the tetradentate was synthesised from (*R*,*R*)-1,2-diaminocyclohexane.[14] Computer generated structures of α-phi (Δ and Λ) were subject to the same ROE restrained MD-MM simulated annealing protocol. Each structure minimised to a single conformation but the Λ-isomer contained many distance violations (Table 1). In particular, H10(Me) to H12e and H10 to H9e were ~15% too long and H12e to H9e 18% too short. In contrast, for the Δ-isomer, no distances varied by more than 5% from the ROE determined values. This difference was reflected in the total restraint energy measured in the final MM calculations for the Δ- and Λ-isomers, which was found to be 50× greater for the latter.

Table 2 shows the coordination bond lengths and angles of the α-phi NMR structure compared to the X-ray structure of α-dpqC.[33] The detailed structural features are very similar. The solution structure of α-phi is perfectly symmetrical about its C_2-axis. The coordination geometry is distorted from octahedral, as the bidentate phi ligand has a small bite angle of 78.9°. A further deviation from octahedral geometry results from the *trans* angles formed by the N atoms on the picolyl groups and the Ru atom (176.9°). This results in a structure where the picolyl rings appear bent away from the phi ligand, as apparent in Fig. 2. This phenomenon is also observed in the crystal structure of [Ru(bpy)$_2$(phi)]$^{2+}$,[34] where the bpy ligands are pinched back away from the phi ligand. This is attributed to the substantial electronic interaction of the phi ligand with the metal centre. The Ru–N(phi) bond lengths (2.09 Å) are in keeping with those determined by X-ray crystallography of Ru and Rh complexes with coordinated phi ligands,[34–36] which show a range of 2.00–2.09 Å. Also consistent with literature results is that the Ru–N(phi) bond lengths are shorter than Ru–N(polypyridyl), typically 2.04–2.23 Å, indicating substantial back-bonding of the phi ligand to the metal centre.[34] The 0.07 Å longer distance observed for the Ru–N(picolyl) bond compared to the X-ray structure of α-dpqC is inconsistent and may reflect a weakness in the ESFF force field. However, with data from the CSD for Ru–pyridine bonds (2.04–2.24 Å, median 2.12 Å[37]) shows a large variation depending on the local environment. The phi ligand forms a plane with the Ru atom, with only a 0.11° buckle between the planes of the two benzene rings. At 25 mM H4 of α-phi is a clean doublet (J = 7.9 Hz) as expected. However, at low concentration (2.5 mM) H4 shows a complex splitting pattern probably due to second order effects caused by buckling of the phi ring system. As the concentration increases, the self-association interaction appears to cause either a flattened ring system or fast exchange resulting in an averaged spectrum. Non-planarity of phi has previously been observed in the crystal structure of Δ-α-[Rh(*R*,*R*-Me$_2$trien)(phi)]$^{3+}$.[38] Overall, however, use of the ESFF force field combined with NMR-derived distance restraints has proved to be a useful method for determining the detailed and accurate structure of a metal complex in solution.

Self-association of phi complexes

NMR spectra of α-phi and β-phi at concentrations from 2.5 mM to 25 mM show dramatic differences (Fig. 3). The former displaying marked offsets with concentration when chemical shifts are plotted as a function of concentration, the phi protons (Fig. 4A) show shielding with increasing concentration and the degree (H1 > H2 > H3 > H4) which is consistent with the protons on the phi ligand furthest from the Ru being affected most by an associated complex. In contrast, the picolyl protons (Fig. 4B) were deshielded by a uniform but small degree. These observations are generally compatible with π–π stacking of the phi ligand but the exponential relationship between concentration and chemical shift suggested oligomerisation rather than dimerisation as previously suggested for the related dpq complex.[10]

For the β isomer, the chemical shift changes were minor (Fig. 3), as several protons on the picolyl and phi rings became only slightly deshielded as the concentration increased (for example, H4, H8, H15 and H14). There was no significant shielding of any protons, indicating that self-association was not occurring for the β isomer for the concentrations tested. A hypothetical β-phi dimer structure shows no potential steric

Table 2 Coordination geometry of the solution structure of Δ-*cis*-α-[Ru(*R*,*R*-picchxnMe$_2$)(phi)]$^{2+}$ compared to the X-ray structures of Λ-*cis*-α-[Ru(*S*,*S*-picchxnMe$_2$)(dpqC)]$^{2+}$

Atoms	Bond angle/°	
	α-phi (NMR)	α-dpqC (X-ray)
N(picolyl)–Ru–N(picolyl)	176.9	176.9
N(bidentate)–Ru–N(amino) (*trans*)	174.9	175.5
N(bidentate)–Ru–N(bidentate)	78.9	78.9
N(amino)–Ru–N(amino)	83.7	81.4
N(bidentate)–Ru–N(amino) (*cis*)	98.9	101.5
Buckle[a]	+0.11	+2.21
	Bond length/Å	
Ru–N(bidentate)	2.09	2.09
Ru–N(picolyl)	2.14	2.07
Ru–N(amino)	2.16	2.16

[a] Buckle is the dihedral angle defined by the two pyridyl rings in the dpqC ligand or the two phenyl rings in phi.

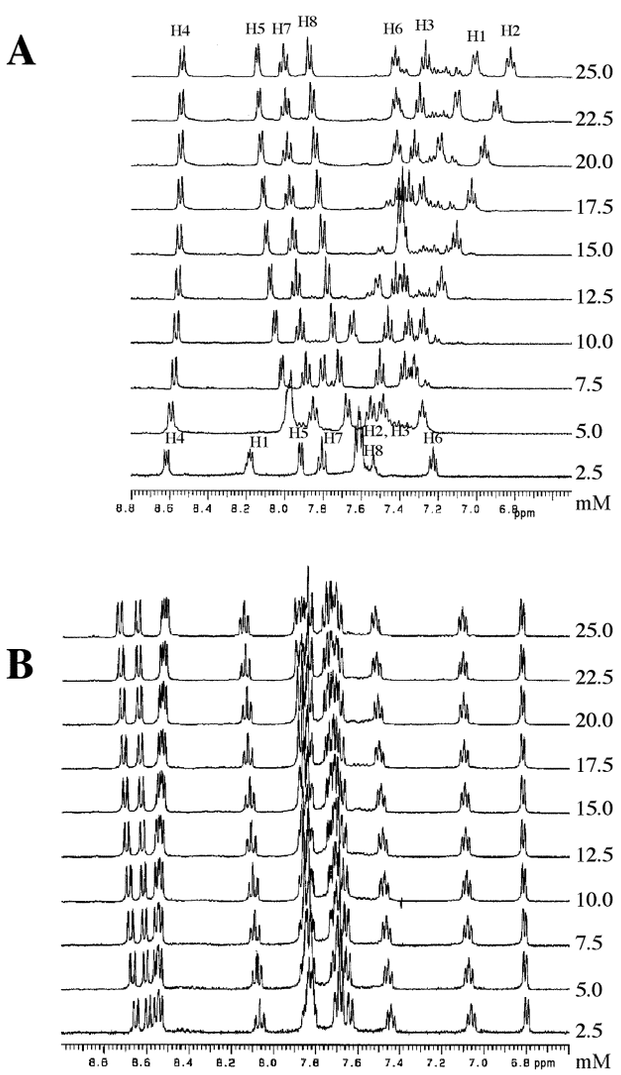

Fig. 3 1D ^{1}H NMR spectra of the aromatic protons of (A) Δ-*cis*-α-[Ru(*R*,*R*-picchxnMe$_2$)(phi)]$^{2+}$ and (B) Δ-*cis*-β-[Ru(*R*,*R*-picchxnMe$_2$)(phi)]$^{2+}$ at varying concentrations (2.5–25 mM, 25 °C, 99.9% D_2O).

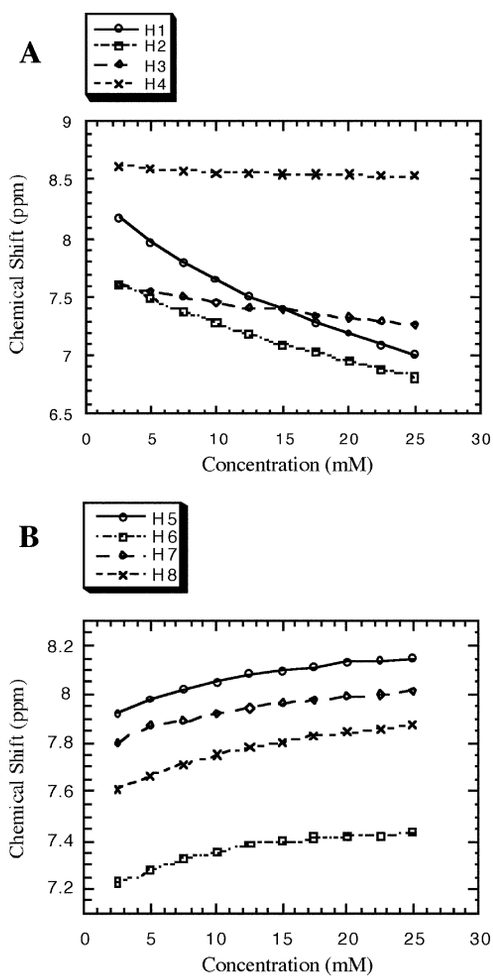

Fig. 4 Chemical shift *vs.* complex concentration line plots for Δ-*cis*-α-[Ru(*R*,*R*-picchxnMe$_2$)(phi)]$^{2+}$ (A) phi protons and (B) picolyl protons.

clashes, but also no stabilising features other than hydrophobic interactions of the two phi ligands to compensate for the mildly repulsive π–π interaction. However, trimeric and higher order structures were impossible due to clashes between the phi and picolyl rings.

In order to quantify intermolecular ROEs to characterise the self-association, it must be demonstrated that the observed ROE cross peaks do not arise from spin diffusion. To this end, several ROESY spectra were acquired (τ_m = 10–300 ms; see ESI). No spin diffusion was noted until a mixing time of 50 ms was applied. At longer τ_m, H8 to H5 correlation begins to appear ($r \approx 5$ Å).

A mixing time of 30 ms was chosen to analyse intermolecular interactions as a compromise between signal intensity and spin diffusion. Fig. 5 shows the aromatic region of the ROESY spectrum at 25 mM. The intermolecular cross peaks at 25 mM that did not appear at 2.5 mM are shown in boxes and occurred between H3–H6, H3–H7, and H4–H6. On the solution structure model of the monomer these distances correspond to 7.69, 8.87, and 6.13 Å intramolecular distances respectively; outside

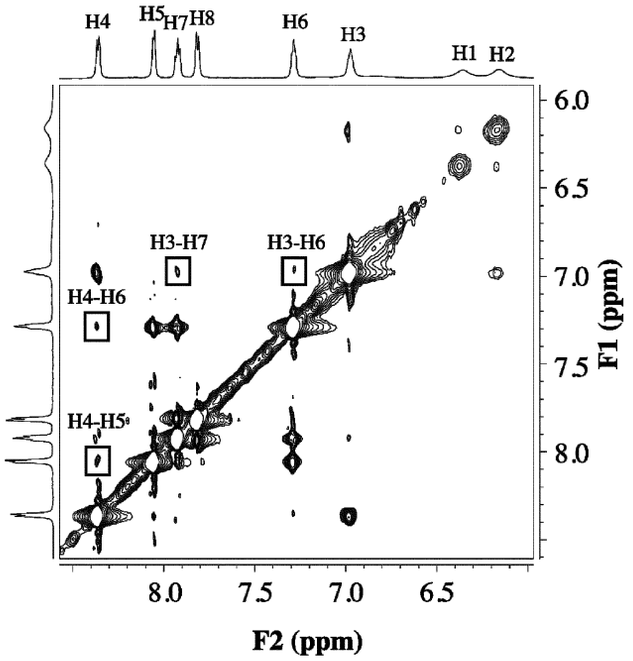

Fig. 5 Aromatic region of a compensated ROESY spectrum of Δ-*cis*-α-[Ru(*R*,*R*-picchxnMe$_2$)(phi)]$^{2+}$ at a concentration of 25 mM (5 °C, τ_m = 30 ms). Intermolecular cross peaks, not seen at 2.5 mM, are shown in boxes.

the range expected for intramolecular ROEs. A cross peak also appeared between H4 and H5 at 25 mM and, although the distance between these atoms is < 5 Å, it does not appear in the spectrum at 2.5 mM, so this cross peak is also labelled and included in the dimer structure calculations. The signals for H1 and H2 at 25 mM were clearly exchange broadened due to the self-association interaction and consequently showed no intermolecular contacts. No intermolecular ROEs were observed from the aromatic protons to the cyclohexyl and methyl protons but it remains possible that many of the remaining ROEs have inter- as well as intra-molecular components at the higher concentration.

As it was not possible to quantify the intermolecular ROEs due to lack of a suitable reference, any distance up to 5 Å was allowed for all observed correlations in the MM simulations. Twenty different starting geometries yielded essentially the same dimer structure shown in Fig. 6. The two complexes overlap at an angle of approximately 35°–37°, which allows for the formation of oligomeric species in solution. Fig. 7 shows an extension of the dimer model into a pseudo-helical oligomeric structure, where the phi ligands are perpendicular to the helical axis and there are ~10 molecules per turn of the helix. The π–π distance between adjacent molecules is ~3.5 Å. The formation

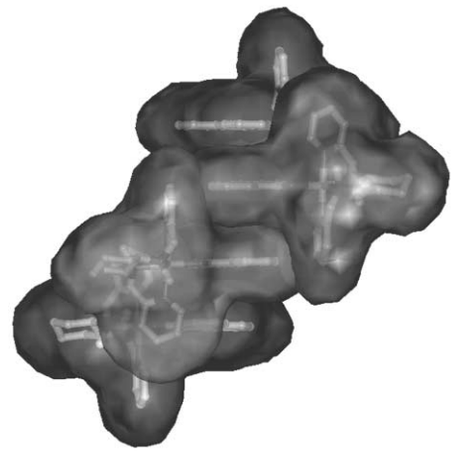

Fig. 7 Hypothetical tetramer of α-phi made from two sets of dimers (Fig. 6). Viewed with Connelly surfaces, it is possible for α-phi to form helix-like oligomers based on PFGLED NMR data.

of this type of structure in solution is entirely consistent with the experiments presented here.

To quantify the self-association, a series of PFGLED spectra were run in water with α-phi concentration of 0, 2.5 and 25 mM. The exponential curve fit for the H_2O resonance resulted in a value of $G^2 = 0.0112 \pm 0.0008$ (T m^{-1})^2. Exponential curve fits for H1, H4 and H7 resonances (Fig. 8) in the α-phi complex at 2.5 mM yielded values of 10.64 ± 0.15, 10.42 ± 0.43 and 10.64 ± 0.20 × 10^{-10} m^2 s^{-1}. At 25 mM, these values reduced to

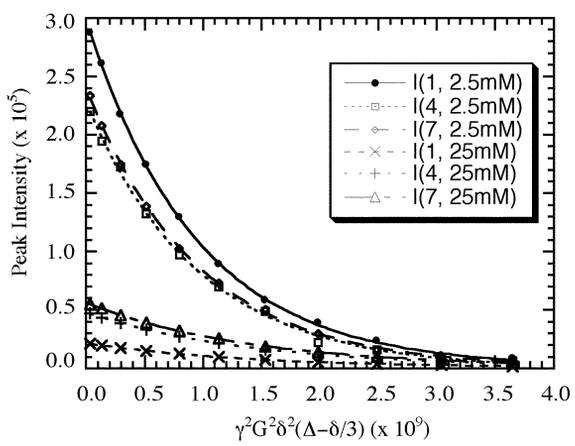

Fig. 8 Peak intensities of three Δ-*cis*-α-[Ru(*R*,*R*-picchxnMe$_2$)(phi)]$^{2+}$ resonances at 2.5 mM and 25 mM, plotted as a function of $\gamma^2G^2\delta^2(\Delta - \delta/3)$. Non-linear least-squares regression of an exponential onto the data yielded the translational diffusion coefficient, D_T, at each concentration.

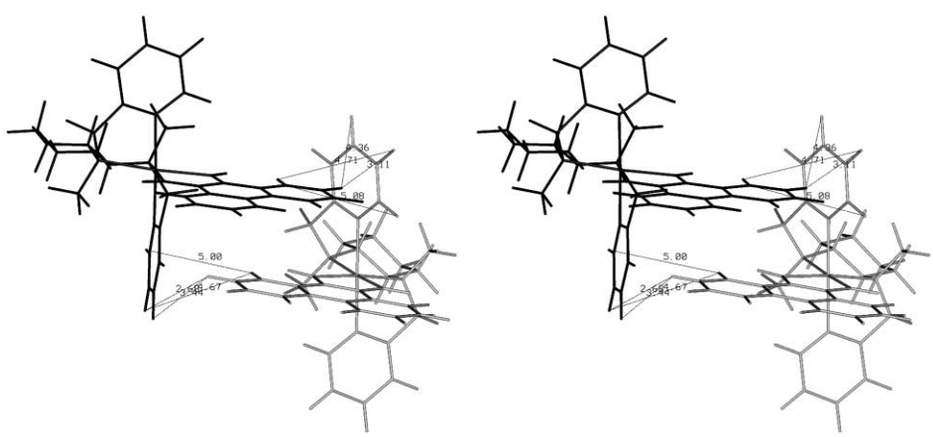

Fig. 6 Stereo-view of the self-associated structure of Δ-*cis*-α-[Ru(*R*,*R*-picchxnMe$_2$)(phi)]$^{2+}$, energy minimised dimer using the intermolecular ROEs shown in Fig. 5 as distance restraints (dotted lines).

7.19 ± 0.23, 7.24 ± 0.10 and 7.29 ± 0.08 × 10^{-10} m^2 s^{-1}, respectively. The average value of D_T at 2.5 mM = (10.57 ± 0.26) × 10^{-10} m^2 s^{-1} and 25 mM = (7.24 ± 0.14) × 10^{-10} m^2 s^{-1} indicated that at the higher concentration, the rate of diffusion through the solvent was substantially slower, consistent with the self-association of the complex. Since, according to eqn. 2, MW ∝ $(1/D_T)^3$, this indicated that the diffusing species at 25 mM was around three times the molecular weight of that at 2.5 mM. Note that this does not imply that at 25 mM the molecule is exclusively a trimer, rather that a distribution of aggregates exists of which a trimer is the average at 25 mM if the molecule is monomeric at 2.5 mM.

Based on this information, the structure of the associated species could be predicted. The results are incompatible with a dimer model stacked end-to-end, as has previously been suggested for the analogous complexes[10,39] as the phi protons would be too far away from the picolyl protons of an adjacent complex to give intermolecular ROEs. If the phi rings were close enough to show ROEs to picolyl protons, then the H1 and H2 protons would move out of the maximum shielded position as indicated by the chemical shift changes shown in Figs. 3 and 4. In addition, a model such as this precludes the formation of additional associated molecules as indicated by the diffusion experiments. A model more consistent with the data is one where a phi complex is rotated about the C_2 axis (formed by the picolyl rings). This model (Fig. 6) allows the formation of intermolecular ROE contacts while keeping the H1 and H2 protons in a maximum shielding zone, and allows the possible formation of oligomeric structures (Fig. 7).

The three experiments described above are consistent with the self-association of α-phi and give complementary information about the nature of the associated species. The chemical shift study indicated that it was the α-conformation of the picchxnMe_2 ligand that is most favourable for self-association. The upfield shift of the phi protons indicated that the protons most shielded by neighbouring aromatic rings were H1 and H2, and to a lesser degree H3 and H4. In contrast, the picolyl protons all showed a downfield shift to a uniform degree. This is consistent with a model in which the phi ligands from different molecules stack on top of each other, resulting in the shielding effects, and the picolyl rings lie equatorial to a phi ligand from a different molecule, resulting in a deshielding effect. The ROESY spectra indicated that there were intermolecular contacts at 25 mM, which were not apparent at 2.5 mM. This led to the conclusion that at 2.5 mM, the molecule existed predominantly as a monomer and at 25 mM, at least two molecules self-associated. Lastly, the translational diffusion measurements indicated that the solute diffused through the solvent more slowly at 25 mM than at 2.5 mM. This is proportional to a three-fold increase in molecular weight at the higher concentration consistent with self-associated oligomerisation.

In conclusion, 2D and PFGLED NMR spectroscopy in conjunction with quantitative ROESY experiments and molecular modelling have proved useful techniques for the structure determination and concentration dependant behaviour of Ru metal complexes in solution.

Acknowledgements

This research was supported by the Australian Research Council and Macquarie University. The authors would like to acknowledge the ARC and Macquarie University for funding of the Macquarie University NMR Facility. We are indebted to R. S. Vagg and K. Vickery for supplying a mixture of Δ-*cis*-α- and Δ-*cis*-β-[Ru(*R*,*R*-picchxnMe_2)(phi)]$^{2+}$. We would also like to thank J. Aldrich-Wright for providing the X-ray coordinates for α-dpqC.

References

1 N. Gupta, G. A. Grover, G. A. Neyhart, W. Liang, P. Singh and H. H. Thorp, *Angew. Chem., Int. Ed. Engl.*, 1992, **31**, 1048.
2 V. W.-W. Yam, K. K.-W. Lo, K.-K. Cheung and R. Y.-C. Kong, *J. Chem. Soc., Chem. Commun.*, 1995, 1191.
3 G. R. Desiraju and A. Gavezzotti, *J. Chem. Soc., Chem. Commun.*, 1989, 621.
4 Y. Masuda and H. Yamatera, *Bull. Chem. Soc. Jpn.*, 1984, **57**, 58.
5 A. Odani, T. Sekiguchi, H. Okada, S. Ishiguro and O. Yamauchi, *Bull. Chem. Soc. Jpn.*, 1995, **68**, 2093.
6 K. R. Koch, C. Sacht and C. Lawrence, *J. Chem. Soc., Dalton Trans.*, 1998, 689.
7 P. R. Mitchell, *J. Chem. Soc. Dalton Trans.*, 1980, 1079.
8 D. B. Davies, L. N. Djimant and A. N. Veselkov, *J. Chem. Soc., Faraday Trans.*, 1996, 383.
9 C. A. Hunter and J. K. M. Sanders, *J. Am. Chem. Soc.*, 1990, **112**, 5525.
10 K. A. Vickery, A. M. Bonin, R. S. Vagg and P. A. Williams, *10th Struct., Motion, Interact. Expression Biol. Macromol., Proc. Conversation Discip. Biomol. Stereodyn.*, eds. R. H. Sharma and M. H. Sarma, Adenine Press, Schenectady NY, 1997, p. 195.
11 T. P. Shields and J. K. Barton, *Biochemistry*, 1995, **34**, 15037.
12 B. P. Hudson, C. M. Dupureur and J. K. Barton, *J. Am. Chem. Soc.*, 1995, **117**, 9379.
13 E. M. Proudfoot, J. P. Mackay and P. Karuso, *Biochemistry*, 2001, **40**, 4867.
14 R. R. Fenton, F. S. Stephens, R. S. Vagg and P. A. Williams, *Inorg. Chim. Acta*, 1991, **182**, 67.
15 J. R. Aldrich-Wright, R. S. Vagg and P. A. Williams, *Coord. Chem. Rev.*, 1997, **166**, 361.
16 E. O. Stejskal and J. E. Tanner, *J. Chem. Phys.*, 1965, **42**, 288.
17 A. J. Dingley, J. P. Mackay, B. E. Chapman, M. B. Morris, P. W. Kuchel, B. D. Hambley and G. F. King, *J. Biomol. NMR*, 1995, **6**, 321.
18 R. L. Haner and T. Schleich, *Methods Enzymol.*, 1989, **176**, 418.
19 P. W. Kuchel and B. E. Chapman, *J. Magn. Reson. Ser. A*, 1993, **101**, 53.
20 C. R. Cantor and P. R. Schimmel, *Biophysical Chemistry, Part II: Techniques for the Study of Biological Structure and Function*, W.H. Freeman, New York, 1980.
21 E. M. Proudfoot, J. P. Mackay, R. S. Vagg, K. A. Vickery, P. A. Williams and P. Karuso, *Chem. Commun.*, 1997, 1623.
22 M. Piotto, V. Saudek and V. Sklenar, *J. Biomol. NMR*, 1992, **2**, 661.
23 A. Bax and D. G. Davis, *J. Magn. Reson.*, 1985, **63**, 207.
24 A. A. Bothner-By, R. L. Stephens, J. Lee, C. D. Warren and R. W. Jeanloz, *J. Am. Chem. Soc.*, 1984, **106**, 811.
25 C. Griesinger, *J. Magn. Reson.*, 1987, **75**, 261.
26 InsightII/Discover3 Molecular Modelling System, Accelrys, San Diego, CA, 1997.
27 G. C. K. Roberts, in *NMR of Macromolecules*, eds. D. Rickwood and B. D. Hames, Oxford University Press, Oxford, 1993.
28 S. Barlow, A. L. Rohl, S. Shi, C. M. Freeman and D. O'Hare, *J. Am. Chem. Soc.*, 1996, **118**, 7578.
29 G. D. van Duyne, R. F. Standaert, P. A. Karplus, S. L. Schreiber and J. Clardy, *Science*, 1991, **252**, 839.
30 S. W. Michnick, M. K. Rosen, T. J. Wandless, M. Karplus and S. L. Schreiber, *Science*, 1991, **252**, 836.
31 W. J. Haelg, L. R. Oehrstroem, H. Rüegger and L. M. Venanzi, *Magn. Reson. Chem.*, 1993, **31**, 677.
32 J. Vogelgesang, A. Frick, G. Huttner and P. Kircher, *Eur. J. Inorg. Chem.*, 2001, 949.
33 J. A. Aldrich-Wright, personal communication, 2002.
34 A. M. Pyle, M. Y. Chiang and J. K. Barton, *Inorg. Chem.*, 1990, **29**, 4487.
35 A. H. Krotz, L. Y. Kuo and J. K. Barton, *Inorg. Chem.*, 1993, **32**, 5963.
36 A. H. Krotz and J. K. Barton, *Inorg. Chem.*, 1994, **33**, 1940.
37 Cambridge Structural Database, Cambridge, 2002.
38 B. P. Hudson and J. K. Barton, *J. Am. Chem. Soc.*, 1998, **120**, 6877.
39 D. Gut, A. Rudi, J. Kopilov, I. Goldberg and M. Kol, *J. Am. Chem. Soc.*, 2002, **124**, 5449.